Applied Catalysis B: Environmental 100 (2010) 264–270

Contents lists available at ScienceDirect

Applied Catalysis B: Environmental

journal homepage: www.elsevier.com/locate/apcatb

# Adsorptive removal of tert-butylmercaptan and tetrahydrothiophene using microporous molecular sieve ETS-10

Gap Soon Jung[a], Dong Ho Park[b,*], Doo Hwan Lee[c], Hyun Chul Lee[d], Suk Bong Hong[e], Hee Chul Woo[a,**]

[a] Department of Chemical Engineering, Pukyung National University, San 100 Yongdang-dong, Nam-gu, Busan 608-739, Republic of Korea
[b] Department of Biomedicinal Chemistry, Inje University, 607 Obang-dong, Gimhae, Gyeongnam 621-749, Republic of Korea
[c] Department of Chemical Engineering, The University of Seoul, 13 Siripdae-gil, Dongdaemun-gu, Seoul 130-743, Republic of Korea
[d] Energy Lab, Samsung Advanced Institute of Technology (SAIT), Samsung Electronics Co., Ltd, San 14, Nongseo-Dong, Giheung-Gu, Yongin 446-712, Republic of Korea
[e] Department of Chemical Engineering and School of Environmental Science and Engineering, POSTECH, San 31 Hyoja-Dong, Nam-gu, Pohang, Gyungbuk 790-784, Republic of Korea

ARTICLE INFO

*Article history:*
Received 2 March 2010
Received in revised form 21 July 2010
Accepted 5 August 2010
Available online 13 August 2010

*Keywords:*
Adsorption
Desulfurization
Cu-exchanged ETS-10
Zeolite

ABSTRACT

The adsorptive removal of tert-butylmercaptan (TBM) and tetrahydrothiophene (THT) in methane gas using microporous molecular sieve ETS-10 was investigated at an ambient temperature and atmospheric pressure. Na,K-ETS-10 and Cu-exchanged Na,K-ETS-10 (Cu-ETS-10) were characterized by X-ray diffractometer (XRD) for the crystalline phase, X-ray fluorescence (XRF) analyzer for the chemical composition, and nitrogen adsorption-isotherm measurement for the BET surface area and porosity, respectively. Posterior to its treatment at 723 K in He atmosphere for 2 h, the Cu(II) in Cu-ETS-10 could be partially autoreduced to Cu(I), which was confirmed by X-ray photoelectron spectroscopy (XPS). The preferential adsorption of THT over TBM on Na,K-ETS-10 and the concurrent adsorption of TBM and THT on Cu-ETS-10 were achieved, which could be explained by the uptake curve in the binary component adsorption, the temperature-programmed desorption, and the apparent activation energy for desorption. The breakthrough sulfur adsorption capacity for both TBM and THT was attained to 2.50 mmol S/g on Cu-ETS-10-0.1(4). This markedly high breakthrough sulfur adsorption capacity on Cu-ETS-10 is unprecedented in removing organic sulfur compounds from fuel gas by adsorption on zeolites.



## 1. Introduction

The adsorptive removal of sulfur compounds in fuel gas is of great significance because sulfur species irreversibly deactivate fuel processing catalysts (supported Ru and Ni catalysts) and cell electrodes for fuel cell, which is one of the most effective energy saving power generation systems [1]. In conversion of gaseous hydrocarbons such as pipeline natural gas and liquefied petroleum gas to hydrogen gas for fuel cell application [2–4], several parts per million (ppm) of organic sulfur compounds incorporated as odorants for the purpose of warning against gas leaks should be removed. Desulfurization of fuel gases by selective sulfur adsorption at an ambient temperature and pressure using various adsorbents, such as metal impregnated oxides [5], porous carbon materials [6,7] and a variety of zeolites [8–16] has attracted a great deal of attention due to its simplicity and adaptability in compact fuel cell systems. Among various metal-exchanged zeolites, Y zeolites exchanged by Group IB transition metals have been reported to be very effective for the removal of organic sulfur compounds such as tetrahydrothiophene (THT), *tert*-butylmercaptan (TBM), and dimethyl sulfide (DMS), as well as thiophene and its derivatives via π interaction between sulfur and d orbital of metal with high adsorptive capacity and selectivity [9,16]. The adsorption strength of THT and TBM on the Na sites is compared with that on the Ag sites in AgNa-Y zeolite [17–20].

Engelhard titanosilicate-10 (ETS-10) is a zeolite-type material composed of microporous titanosilicate containing pseudolinear chains of corner sharing $TiO_6$ octahedra that are embedded in a tetrahedral $SiO_4$ framework, which leads to the formation of a three-dimensional 12-membered ring pore system [21]. ETS-10 has attracted increasing attention due to its high ion-exchange capacity, basicity of framework, and presence of nanomolecular wire in the framework [22].

In this work, we prepared ETS-10. And then, as-prepared ETS-10 was transformed to Cu-ETS-10 through ion exchange under the conditions of various pH values and $Cu(NO_3)_2$ concentrations to develop a new promising adsorbent for the removal of sulfur compounds. The effect of copper ion on the adsorptive properties of TBM and THT in the ellipsoidal pore of ETS-10 having a pore size of 5 Å × 8 Å was investigated. For the case of Na,K-ETS-

* Corresponding author. Tel.: +82 55 320 3224; fax: +82 55 321 9718.
** Corresponding author. Tel.: +82 51 629 6436; fax: +82 51 629 6429.
*E-mail addresses:* chempdh@inje.ac.kr (D.H. Park), woohc@pknu.ac.kr (H.C. Woo).

0926-3373/$ – see front matter © 2010 Elsevier B.V. All rights reserved.
doi:10.1016/j.apcatb.2010.08.002

10, the preferential adsorption of THT over TBM was observed, while, interestingly, the concurrent adsorption of THT and TBM on Cu-ETS-10 was observed in the uptake curve in a binary component adsorption measurement of THT and TBM. These different adsorption characteristics in the Na,K-ETS-10 and Cu-ETS-10 were analyzed by the apparent activation energy for desorption and the temperature-programmed desorption (TPD). Noticeably, the breakthrough adsorption capacity for both TBM and THT on Cu-ETS-10 was 2.50 mmol S/g (0.75 mmol S/g for the TBM, 1.75 mmol S/g for the THT), which is higher than that in previous best results from Y zeolite and metal-exchanged Y zeolite [19,20,23].

## 2. Experimental

### 2.1. Preparation of adsorbents

The titanosilicate molecular sieve Na,K-ETS-10 was synthesized using the procedure reported by Das et al. [24]. In a typical synthesis, a solution of 18.7 g NaOH (Katayame, 96%) in 100 g distilled water was added to a solution of 140 g sodium silicate (Junsei, 38% $SiO_2$, 19% $Na_2O$, 43% $H_2O$) in 100 g distilled water with vigorously stirring. This was followed by a dropwise addition of a solution of 12 mL $TiCl_4$ (Junsei, 99%) in 54 mL HCl (Osaka, 35%) into the silicate–NaOH–$H_2O$ mixture with rapid stirring. A solution of 12.1 g KF (Junsei, 98%) in 20 mL distilled water was then added into the above mixture also with vigorous stirring. The final pH of this gel mixture was in the range between 11.4 and 11.5, and the molar composition was 1.0 $TiO_2$:5.7 $SiO_2$:6.0 $Na_2O$:1.9 KF:144 $H_2O$. The resultant was stirred until to be homogenous and crystallized in a stainless-steel autoclave (136 mL) under autogenous pressure at 473 K for 18 h. The final resulting product was cooled down to room temperature, filtered and washed with distilled water until the pH of the filtrate reached 7.0 and then dried at 353 K overnight.

The Na and K cations in Na,K-ETS-10 were ion exchanged into Cu cations with varying the concentrations of $Cu(NO_3)_2$ aqueous solution and pH values. The concentrations of $Cu(NO_3)_2$ aqueous solution were 0.01, 0.05, 0.1 and 0.5 M, respectively. The pH values of the solution were adjusted to be 3, 4, 11, and 12, respectively, using $NH_4OH$ or $HNO_3$ while monitoring with a pH meter (pH meter 720P, Istek-Korea). Then, 1.0 g of Na,K-ETS-10 was added into 140 mL of the prepared solution at 303 K by shaking in a water bath for 8 h, and the adsorbent was washed in distilled water and dried at 353 K overnight. These final Cu-exchanged Na,K-ETS-10 samples are referred to as Cu-ETS-10-*m*(*n*), where *m* stands for the concentration of $Cu(NO_3)_2$ aqueous solution, and *n* for the pH value adjusted by $NH_4OH$ or $HNO_3$.

### 2.2. Characterization of adsorbents

The crystalline phase of Na,K-ETS-10 and Cu-ETS-10 was identified by powder X-ray diffractometer (XRD, a Philips X'pert-MPD) with graphite-monochromatized Cu $K_\alpha$ ($\lambda$ = 1.5406 Å) radiation operated at 40 kV and 30 mA. The spectra were taken with a scanning speed of 4°/min over the range of 2$\theta$ from 5° to 80°.

$N_2$ adsorption-isotherm measurements were carried out to calculate the BET surface area and porosity of adsorbents with a BELSORP-MAX apparatus at a liquid $N_2$ temperature of 77 K. Prior to analysis, the sample was vacuum-treated at 703 K for 6 h. The specific micropore volume was determined by the *t*-plot method [25].

The elemental composition analysis of ETS-10 samples was carried out using a X-ray fluorescence (XRF, SHIMADZU-Japan XRF-1700) analyzer to obtain Ti, Si, Na, K, and Cu content.

X-ray photoelectron spectroscopy (XPS) was used to investigate the oxidation states of the copper species using a MultiLab 2000 spectrometer with an analysis chamber base pressure of $10^{-8}$ Torr with Mg $K_\alpha$ (1254.6 eV) for the X-ray source. The XPS measurement of Cu-ETS10-0.1(4) was performed after pretreatment in He at 723 K for 2 h, and after adsorption of sulfur compounds at room temperature posterior to He treatment.

### 2.3. Adsorption experiment

The sulfur adsorption uptake runs were carried out in a small tubular reactor (inner diameter: 4 mm) containing 40 mg of adsorbent at 303 K under atmospheric pressure. Prior to their adsorption, the adsorbents were pretreated at 723 K for 2 h in 50 mL/min He. After the adsorbents were cooled to 303 K, a simulated gas comprising 69.8 ppmv THT and 29.9 ppmv TBM balanced with $CH_4$ was passed through them at a flow rate of 50 mL/min. The concentrations of THT and TBM in the inlet and outlet gases were analyzed by a gas chromatograph (HP-5890) equipped with an HP-1 capillary column (length of 30 m, inner diameter of 0.32 mm, film thickness of 0.25 μm) and a flame ionization detector (FID). The breakthrough uptake was defined as the amount of sulfur adsorbed on the adsorbent before the sulfur species is detected by FID (lower detection limit of FID = ~0.1 ppm S). The total uptake was defined as the amount of sulfur compound adsorbed on the adsorbent until sulfur concentration in the effluent equilibrated to that in the feed stream. This can be calculated by the following formula [20].

$$\text{Total capacity} = \frac{F}{M}\int_0^t (C_{\text{in}} - C_{\text{ef}})dt \quad (1)$$

In this equation, *F* is the molar flow rate of the feed, *M* is the weight of the adsorbent, $C_{\text{in}}$ is the sulfur concentration in the feed, $C_{\text{ef}}$ is the sulfur concentration in the effluent, and *t* is the time.

The temperature-programmed desorption (TPD) of THT ($m/e$ = 60) and TBM ($m/e$ = 41) [26] adsorbed on the adsorbents was conducted over 40 mg of adsorbent posterior to the adsorption run. The adsorbent was purged for 1 h in 50 mL/min He at 303 K, and then TPD was carried out with raising temperature from 303 to 773 K at a rate of 10 K/min in 50 mL/min He [27]. The species desorbed in TPD runs were analyzed by a mass spectrometer (HPR 20).

### 2.4. Activation energy

The apparent activation energy ($E_d^*$) for organic sulfur compounds can be calculated by following equation reported by Cvetanovic and Amenomiya [28], which offers correlation of the apparent activation energy with the temperature of maximum desorption rate and the heating rate of desorption.

$$\log\left(\frac{T_m^2}{\beta}\right) = \frac{E_d^*}{2.303RT_m} + \log\left(\frac{E_d^*}{RA}\right) \quad (2)$$

where $T_m$ is the temperature (K) at maximum peak point in the desorption curve, $\beta$ is the heating rate (K/min), $E_d^*$ is the apparent activation energy (kJ/mol), *R* is the gas constant, and *A* is an index representing the argument. Therefore, $E_d^*$ can be determined from the relationship between $\log(T_m^2/\beta)$ and $1/T_m$ in which $T_m$ can be measured as a function of $\beta$.

The apparent activation energies for the desorption of THT and TBM on Na,K-ETS-10 and Cu-ETS-10-0.1(4) were measured using the samples pre-saturated with a stream of 100 ppm of THT or 99.6 ppm of TBM balanced with $CH_4$, respectively. A 40 mg of adsorbent was pretreated in 50 mL/min of He flow at 723 K for 2 h followed by cooling to room temperature. After saturation of the single component adsorbate (THT or TBM) at 303 K followed by He purging at 303 K, the adsorbate was desorbed in the range from

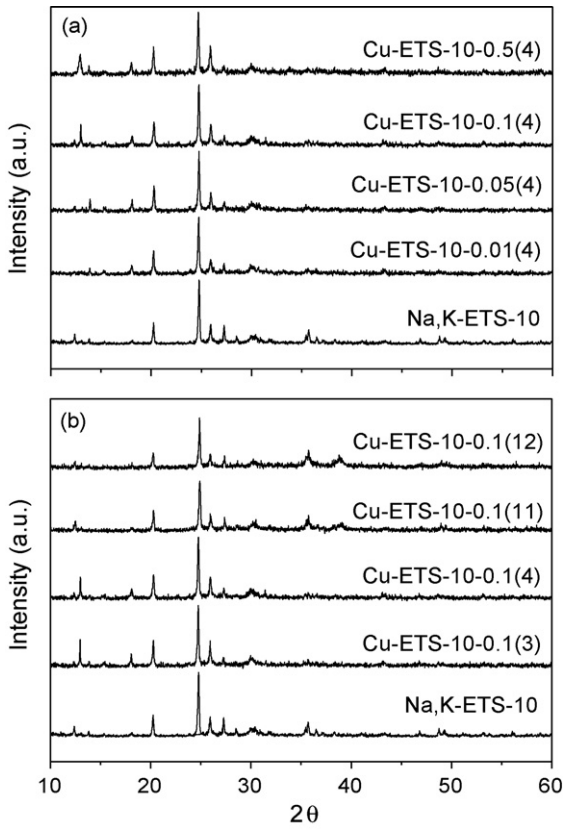


**Fig. 1.** XRD patterns of Na,K-ETS-10 and Cu-ETS-10 (a) with various Cu exchange levels and (b) treated at various pH.

303 to 773 K at heating rates of 2, 5, 8, 10, and 15 K/min, respectively. The apparent activation energy was obtained from the plot of $\log(T_m^2/\beta)$ versus $1/T_m$.

## 3. Results and discussion

### 3.1. Characteristics of adsorbents

Na,K-ETS-10 was ion exchanged with various concentrations of $Cu(NO_3)_2$ aqueous solutions (0.01, 0.05, 0.1, and 0.5 M) at a fixed pH of 4.0. Moreover, Na,K-ETS-10 was ion exchanged with 0.1 M $Cu(NO_3)_2$ solution under various pH conditions (3, 4, 11, and 12) controlled by $NH_4OH$ and $HNO_3$. Fig. 1 shows XRD patterns of Na,K-ETS-10 and Cu-ETS-10 with various Cu exchange levels at a fixed pH of 4.0 (Fig. 1a) and treated with various pH conditions at a fixed $Cu(NO_3)_2$ concentration of 0.1 M (Fig. 1b). The results of XRD patterns for Na,K-ETS-10 and Cu-ETS-10 exhibit characteristic peaks corresponding to the Na,K-ETS-10 crystallographic structure at degree of $2\theta$ values of 6.0, 12.3, 20.1, 24.7, and 27.1 [29]. There are no characteristic peaks for crystalline phases other than ETS-10.

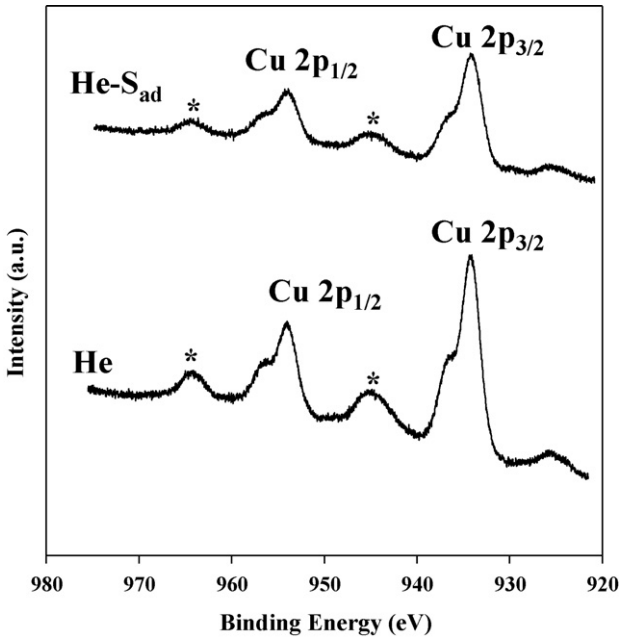


**Fig. 2.** XPS spectra of copper species in Cu-ETS-10-0.1(4) (a) treated in He at 723 K for 2 h and (b) adsorbed sulfur compound at room temperature posterior to He treatment.

Table 1 lists the molar ratios of (Na + K)/Ti, Cu/Ti, (Na + K + Cu)/Ti, and Si/Ti of the adsorbents, which were calculated using the molar composition obtained by XRF. The level of Cu exchange with Na(I) and K(I) in Na,K-ETS-10 under acidic conditions is higher than that under basic conditions, as shown in Table 1. Especially, the ion exchange of Na(I) and K(I) with the copper species at a pH value of 4 is more effective than those at other pH values. At pH 4, the amount of copper incorporated in Na,K-ETS-10 increased with higher $Cu(NO_3)_2$ concentrations. Except for Cu-ETS-10-0.1(3) and Cu-ETS-10-0.5(4), the (Na + K + Cu)/Ti molar ratio of the adsorbents is nearly unity, which is similar to that of Na,K-ETS-10, indicating that Na(I) and K(I) are substituted by equivalent copper species such as $Cu_2(OH)_2$(II) or CuOH(I) generated through the hydrolysis of Cu(II) in an aqueous solution. In the case of Cu-ETS-10-0.5(4), the Cu/Ti and (Na + K + Cu)/Ti molar ratios are 1.55 and 1.70, respectively, indicating that an excessive amount of copper was incorporated into ETS-10 in the form of a copper oxide phase. Most of the Cu ions are present in the Cu(I) oxidation state by autoreduction from Cu(II) to Cu(I) during treatment at 723 K under He atmosphere, as reported by Takahashi et al. [30].

XPS spectroscopy makes it possible to evaluate the oxidation state of the copper ions in Cu-ETS-10. Fig. 2 shows the Cu 2p spectra of Cu-ETS-10-0.1(4) treated (a) in He at 723 K for 2 h and (b) in He at 723 K for 2 h followed by the adsorption of the sulfur compounds. The peak at 932.1 and 951.9 eV of the XPS spectra can be assigned to the binding energy of the Cu $2p_{3/2}$ and Cu $2p_{1/2}$ states of Cu(I), respectively. Both of the shoulders with a higher binding energies

**Table 1**
The molar composition of Na,K-ETS-10 and Cu-ETS-10 zeolites through XRF analysis.

| Sample name | (Na + K)/Ti (mol/mol) | Cu/Ti (mol/mol) | (Na + K + Cu)/Ti (mol/mol) | Si/Ti (mol/mol) |
|---|---|---|---|---|
| Na,K-ETS-10 | 1.00 | 0.00 | 1.00 | 3.07 |
| Cu-ETS-10-0.1(3) | 0.21 | 0.58 | 0.79 | 4.11 |
| Cu-ETS-10-0.1(4) | 0.22 | 0.71 | 0.93 | 4.40 |
| Cu-ETS-10-0.1(11) | 0.57 | 0.47 | 1.04 | 4.08 |
| Cu-ETS-10-0.1(12) | 0.56 | 0.48 | 1.04 | 3.99 |
| Cu-ETS-10-0.01(4) | 0.26 | 0.69 | 0.95 | 4.03 |
| Cu-ETS-10-0.05(4) | 0.22 | 0.77 | 0.98 | 4.10 |
| Cu-ETS-10-0.5(4) | 0.14 | 1.55 | 1.70 | 4.52 |

**Table 2**
Textural properties of Na,K-ETS-10 and Cu-ETS-10 zeolites.

| Sample name | Pore volume ($cm^3/g$) | | Surface area ($m^2/g$) |
|---|---|---|---|
| | Total pore[a] | Micropore[b] | |
| Na,K-ETS-10 | 0.18 | 0.15 | 400 |
| Cu-ETS-10-0.1(3) | 0.18 | 0.15 | 394 |
| Cu-ETS-10-0.1(4) | 018 | 0.15 | 391 |
| Cu-ETS-10-0.1(11) | 0.18 | 0.13 | 359 |
| Cu-ETS-10-0.1(12) | 0.17 | 0.13 | 346 |
| Cu-ETS-10-0.01(4) | 0.17 | 0.14 | 379 |
| Cu-ETS-10-0.05(4) | 0.17 | 0.14 | 375 |
| Cu-ETS-10-0.5(4) | 0.15 | 0.12 | 315 |

[a] Total pore volume at $P/P_0 = 0.99$.
[b] Measured from *t*-plot method.

than the Cu $2p_{3/2}$ and Cu $2p_{1/2}$ states of Cu(I) are attributable to Cu(II) and the characteristic shake-up satellite peaks, which are asterisked, are resulted from Cu(II). From the deconvolution of the peaks in XPS spectra, we could confirm that the Cu species existed as Cu(I) oxidation state at about 70 percent of the total Cu species, which might be autoreduced by the thermal treatment with He flow.

The textural properties of Na,K-ETS-10 and Cu-ETS-10 zeolites are listed in Table 2. The total pore volume calculated at $P/P_0 = 0.9$ of nitrogen adsorption isotherm, the micropore volume measured from the *t*-plot method, and the BET surface area of Na,K-ETS-10 are 0.18 $cm^3/g$, 0.15 $cm^3/g$, and 400 $m^2/g$, respectively. The total pore volumes of the Cu-ETS-10 samples are in the range of 0.17–0.18 $cm^3/g$, except for Cu-ETS-10-0.5(4) which shows much low value of 0.15 $cm^3/g$. The surface areas and micropore volumes of the Cu-ETS-10 samples treated under basic conditions are lower than those treated under acidic conditions, indicating that part of the framework structure of ETS-10 may have collapsed in the basic solution. In the case of Cu-ETS-10-0.5(4), the pore volume and surface area decreased, which resulted from the blockage of the micropore in the ETS-10 framework by copper oxide species transformed from excessive copper ions.

### 3.2. Adsorption uptake of TBM and THT on adsorbents

After the adsorbents were activated at 723 K for 2 h under He flow of 50 mL/min, a gas stream containing THT and TBM in $CH_4$ gas was passed through a fixed bed column, and the outlet concentration was monitored as a function of time. The breakthrough uptake is defined as the amount of sulfur compound adsorbed on the adsorbent before the sulfur compound in the effluent is detected by FID. The total uptake is defined as the amount of sulfur compound adsorbed on the adsorbent up to the point where the sulfur concentration in the effluent was equal to that in the feed stream.

Table 3 shows the sulfur adsorption uptake, measured using a mixture of 29.7 ppmv TBM and 69.4 ppmv THT balanced with a $CH_4$ gas on Cu-ETS-10-0.1 treated with different pH conditions. The adsorption properties of TBM and THT on Cu-ETS-10-0.1(4), which is ion exchanged with 0.1 M $Cu(NO_3)_2$ solution at pH 4, are superior to those obtained in the samples prepared at other pH values.

**Table 3**
Adsorption uptake of TBM and THT on Na,K-ETS-10 and Cu-ETS-10 treated at various pH.

| Sample name | Breakthrough uptake (mmol S/g) | | Total uptake (mmol S/g) | |
|---|---|---|---|---|
| | TBM | THT | TBM | THT |
| Na,K-ETS-10 | 0.30 | 1.06 | 0.04 | 1.48 |
| Cu-ETS-10-0.1(3) | 0.37 | 0.87 | 0.58 | 1.39 |
| Cu-ETS-10-0.1(4) | 0.75 | 1.75 | 0.89 | 2.10 |
| Cu-ETS-10-0.1(11) | 0.57 | 1.34 | 0.71 | 1.71 |
| Cu-ETS-10-0.1(12) | 0.59 | 1.38 | 0.80 | 1.89 |

**Table 4**
Adsorption uptake of TBM and THT on Cu-ETS-10 with various copper exchange levels.

| Sample name | Breakthrough uptake (mmol S/g) | | Total uptake (mmol S/g) | |
|---|---|---|---|---|
| | TBM | THT | TBM | THT |
| Cu-ETS-10-0.01(4) | 0.51 | 1.18 | 0.78 | 1.79 |
| Cu-ETS-10-0.05(4) | 0.71 | 1.65 | 0.82 | 1.91 |
| Cu-ETS-10-0.1(4) | 0.75 | 1.75 | 0.89 | 2.10 |
| Cu-ETS-10-0.5(4) | 0.32 | 0.75 | 0.66 | 1.47 |

Table 4 lists the results of the adsorption experiments of TBM and THT, measured also using the mixture of 29.7 ppmv TBM and 69.4 ppmv THT balanced with a $CH_4$ gas on for Na,K-ETS-10 and Cu-ETS-10 with different Cu loadings. The breakthrough uptakes of TBM and THT in Na,K-ETS-10 are 0.30 (22%) and 1.06 (78%) mmol S/g, respectively. The ratio of the adsorbed amount of TBM to that of THT is different from that in the feed gas stream (30%:70%). This reflects that THT can adsorb preferentially over TBM into the microporous space of Na,K-ETS-10 in a binary component adsorption of THT and TBM. The total uptakes of TBM and THT in Na,K-ETS-10 are 0.04 and 1.48 mmol S/g, respectively. Posterior to the occurrence of breakthrough in the binary component adsorption, THT adsorbed on the adsorption sites with the concomitant desorption of TBM until THT occupied on most of the adsorption sites in Na,K-ETS-10. The breakthrough and total uptakes of TBM and THT on Cu-ETS-10, except for Cu-ETS-10-0.5(4), are higher than those of Na,K-ETS-10. With increase in the copper exchange level, except in Cu-ETS-10-0.5(4), the adsorbed amount of TBM and THT on Cu-ETS-10 increases. As the Cu(I) ion with $3d^{10}$ electron configuration is a softer acid than alkali metal ions such as Na(I) and K(I), the interaction of Cu ion with sulfur compounds as a soft base can be strengthened. This leads to more closely packing of the sulfur compounds in Cu-ETS-10 than in Na,K-ETS-10. Noticeably, differ from the TBM and THT uptake in Na,K-ETS-10, the ratio of the adsorbed amount of TBM and THT (roughly 30%:70%) remains similar to that in the feed gas stream. In Cu-ETS-10, TBM and THT were adsorbed simultaneously, differ from Na,K-ETS-10, maximizing its sulfur adsorption capacity. For an example, the TBM uptake on Cu-ETS-10-0.1(4) is not affected by the co-presence of THT, and the breakthrough sulfur adsorption capacity for both TBM and THT is 2.50 mmol S/g (0.75 mmol S (TBM)/g, 1.75 mmol S (THT)/g). This value is superior to Y zeolites and considered as the best sulfur capacity reported thus far (2.15 mmol S (THT,TBM)/g for AgNa-Y and 0.90 mmol S (THT)/g for H-USY) [19,20].

Fig. 3 shows the uptake curves obtained using a single TBM or THT component adsorption on Na,K-ETS-10 and Cu-ETS-10-0.1(4). In the uptake curves in Fig. 3, the sulfur concentration in the effluent (denoted as *C*) was normalized with that in the feed stream (denoted as $C_0$) and plotted as a function of time. The breakthrough and total uptake amounts of both TBM and THT on Cu-ETS-10-0.1(4) are slightly higher than those on Na,K-ETS-10.

Fig. 4 shows the uptake curves for the binary component feed stream of TBM and THT on Na,K-ETS-10 and Cu-ETS-10-0.1(4). As illustrated in Fig. 4a for TBM and THT adsorption on Na,K-ETS-10, both TBM and THT adsorbed on the empty adsorption sites of low adsorbate coverage at the same time at the beginning. Prior to the breakthrough of TBM, neither TBM nor THT appeared in the effluent. As the adsorbate coverage on the surface increased, TBM breakthrough began and its concentration in the effluent increased reaching about 2.5 times higher than that in the inlet gas stream, and then finally leveled off to the same concentration in the feed stream ($C/C_0 = 1$). Adsorption characteristics of THT differed com-

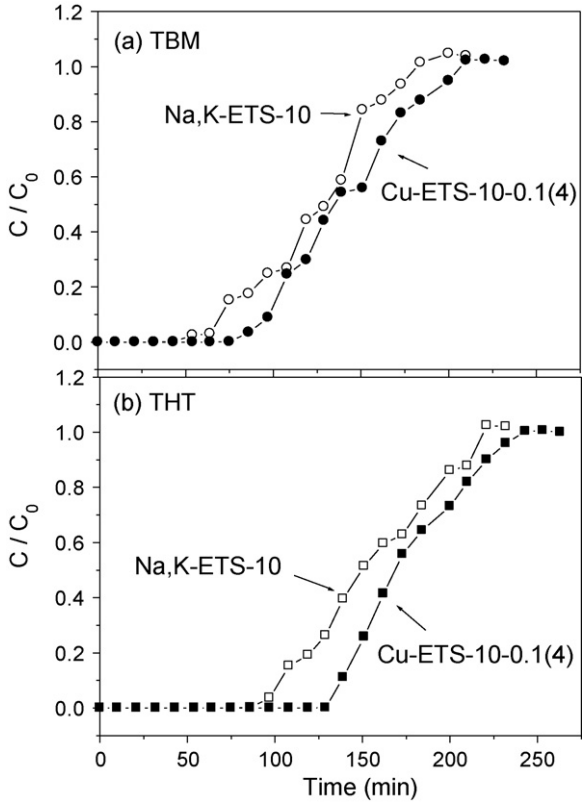


**Fig. 3.** Breakthrough curve in a single component adsorption of (a) TBM and (b) THT on Na,K-ETS-10 and Cu-ETS-10-0.1(4).

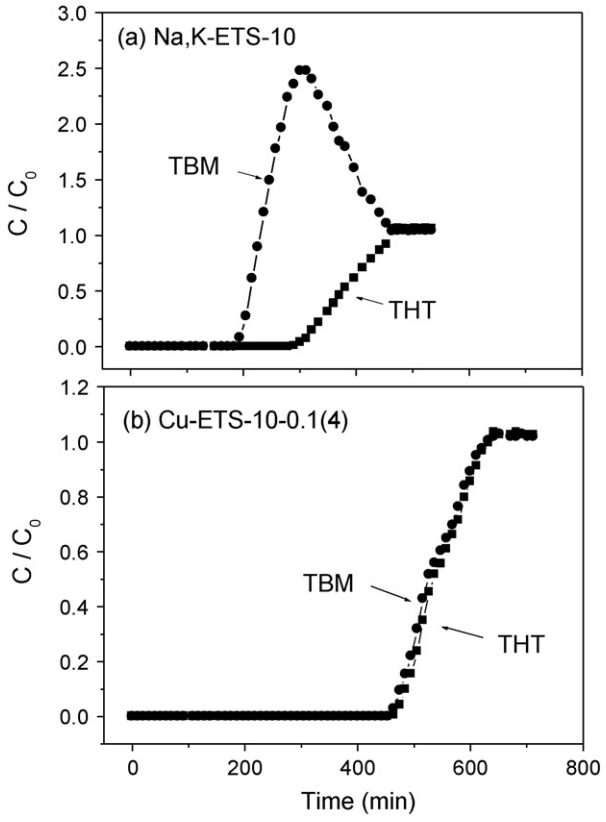


**Fig. 4.** Breakthrough curve in binary component adsorption of TBM and THT on (a) Na,K-ETS-10 and (b) Cu-ETS-10-0.1(4).

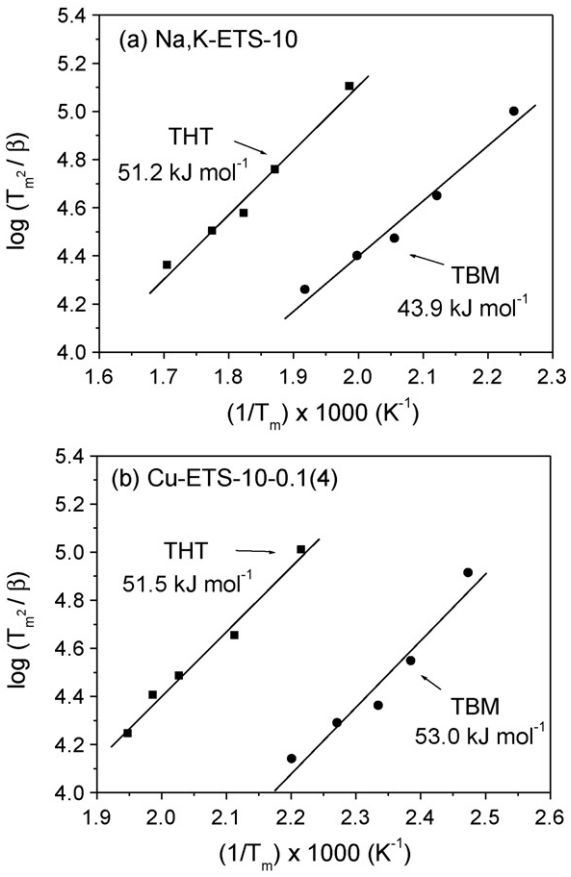


**Fig. 5.** Plot of $\log(T_m^2/\beta)$ against $(1/T_m) \times 1000$ ($K^{-1}$) for TBM and THT on (a) Na,K-ETS-10 and (b) Cu-ETS-10-0.1(4).

pletely from TBM. Even after breakthrough of TBM in the effluent gas, THT was still being taken up. And then, its concentration in the effluent began to increase and reached gradually to the value of inlet gas stream ($C/C_0 = 1$). The integration area of TBM uptake curve in the region exceeding the feed gas concentration level ($C/C_0 = 1$) was nearly the same with that in the region below level. This reflects that the desorbed amount of TBM is nearly the same with the adsorbed one, which results in 0.04 mmol S/g of the total uptake amount on Na,K-ETS-10 as shown in Table 3. The THT adsorption amount is 1.48 mmol S/g, and this nearly the same with the total adsorption amount of THT and TBM on Na,K-ETS-10 at the time of TBM breakthrough occurred. As the adsorption sites were saturated by TBM and THT, THT molecules diffused in the pores of Na,K-ETS-10 lead to the desorption of weakly adsorbed TBM molecules resulting in the preferential THT adsorption on Na,K-ETS-10. This indicates that THT and TBM adsorption occur at the same adsorption sites on Na,K-ETS-10, and its adsorptive interaction with THT is much stronger than that with TBM. The similar preferential adsorption was reported in the adsorptive removal of THT and TBM using AgNa-Y zeolite, where THT dominantly adsorbed on AgNa-Y resulting in an almost 100% overall selectivity for THT over TBM [20]. Markedly differ from the sulfur uptake on Na,K-ETS-10 for a binary mixture of TBM and THT, an introduction of copper ion in the framework of Na,K-ETS-10 lead to concurrent adsorption of TBM and THT even at high coverage of the species on the adsorbent surface without desorption of TBM as shown in Fig. 4b. From this result it can be deduced that the adsorption strength of TBM on Cu-ETS-10 is comparable to that of THT, and the adsorption energy of TBM on the adsorption site in Cu-ETS-10 is higher than that of Na,K-ETS-10.

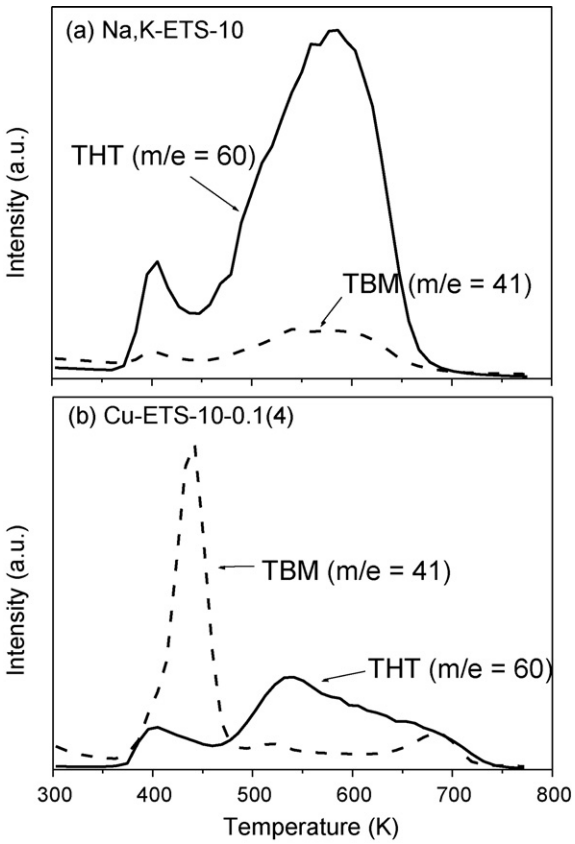


**Fig. 6.** TPD profiles in binary components of TBM and THT on (a) Na,K-ETS-10 and (b) Cu-ETS-10-0.1(4). The numbers in the figures are the mass numbers detected. Conditions: 0.04 g sample weight, 10 K/min heating rate, and 50 mL/min He.

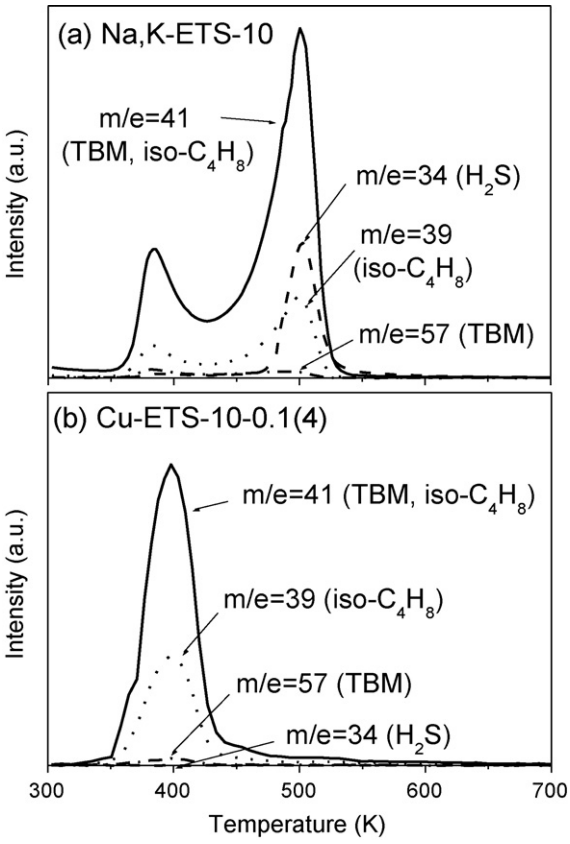


**Fig. 7.** The ionic current during TPD of TBM adsorbed on (a) Na,K-ETS-10 and (b) Cu-ETS-10-0.1(4).

### 3.3. The apparent activation energy for desorption

The apparent activation energy for desorption ($E_d^*$) of TBM and THT adsorbed on ETS-10 is an indirect evidence of the adsorption strength of sulfur compounds, which can be obtained from Eq. (2) by plotting $\log(T_m^2/\beta)$ against $(1/T_m)$ as a function of heating rate, $\beta$. The results are shown in Fig. 5. The $E_d^*$ value for TBM and THT on Na,K-ETS-10 is 43.9 and 51.2 kJ/mol, respectively. It reflects that the adsorption strength of THT is higher than that of TBM, which induce the preferential adsorption of THT over TBM on Na,K-ETS-10. The $E_d^*$ value for TBM and THT on Cu-ETS-10-0.1(4) is 53.0 and 51.5 kJ/mol, respectively, and these comparable values lead in turn to the concurrent adsorption of TBM and THT on Cu-ETS-10-0.1(4).

### 3.4. Temperature-programmed desorption of THT and TBM

Fig. 6a shows the TPD curve of THT and TBM after reaching the equilibrium state for the binary component adsorption on Na,K-ETS-10. The results show that desorption of TBM ($m/e = 41$, $C_3H_5$, the main fragment of TBM) occurred at 400 and 540 K with a very weak peak. On the other hand, desorption of THT ($m/e = 60$, $C_2H_4S$, the main fragment of THT) showed strong peaks at 400 and 580 K. It reflects that the adsorbed amount of THT at adsorption equilibrium in the binary component adsorption system in Na,K-ETS-10 is much higher than that of TBM, and this agrees with the adsorption uptake results. TBM and THT adsorbed competitively on the sorption site in Na,K-ETS-10, although the adsorption strength of THT on the site was much higher than that of TBM. Fig. 6b shows that the TPD patterns of THT and TBM co-adsorbed on Cu-ETS-10-0.1(4). Desorption of TBM ($m/e = 41$) showed a sharp peak at 440 K and a relatively weak peak at 690 K. On the other hand, desorption of THT ($m/e = 60$) showed broad peaks at 390 and 540 K. These results significantly differ from those obtained on Na,K-ETS-10. Noticeably, all the desorption peaks of TBM on Cu-ETS-10 were shifted largely into a higher temperature region compared with those on Na,K-ETS-10 (from 400 to 440 K, from 540 to 690 K), indicating the adsorption strength of TBM on Cu-ETS-10 is much higher than that in Na,K-ETS-10. On the contrast, for the case of THT on Cu-ETS-10, all the desorption peaks were shifted slightly into a lower temperature region than those on Na,K-ETS-10 (from 400 to 390 K, from 580 to 540 K), also reflecting the adsorption strength of THT on Cu-ETS-10 is similar with that in Na,K-ETS-10. Those results might be reflected in the apparent activation energy of desorption for TBM and THT on the Na,K-ETS-10 and Cu-ETS-10, respectively. That is, the apparent activation energy for TBM markedly increased on Cu-ETS-10 as 53.0 kJ/mol compared with 43.9 kJ/mol on Na,K-ETS-10, while the apparent activation energy for THT seemed to similar (51.5 kJ/mol on Cu-ETS-10 and 51.2 kJ/mol on Na,K-ETS-10). Thus, the increased adsorption strength of TBM on Cu-ETS-10 would be attributed to the concurrent adsorption of TBM and THT for sulfur adsorption with the binary mixture feed stream.

Fig. 7 shows the TPD profiles of TBM adsorbed on (a) Na,K-ETS-10 and (b) Cu-ETS-10-0.1(4) in a single component adsorption. The intensity of the peaks of $m/e = 41$ and 39 (fragment of iso-$C_4H_8$) and 34 ($H_2S$) on Cu-ETS-10-0.1(4) in the profile is weaker than that on Na,K-ETS-10. Fig. 8 displays the TPD profiles of THT adsorbed on (a) Na,K-ETS-10 and (b) Cu-ETS-10-0.1(4) in a single component adsorption. Similarly, the intensity of the TPD peaks of THT on Cu-ETS-10-0.1(4) is also weaker than that on Na,K-ETS-10, indicating that the sulfur compounds are more strongly adsorbed on the Cu ion sites in Cu-ETS-10-0.1(4) compared with those on Na,K-ETS-10. It would be reasonable to deduce that the oleffinic fragments, such as n-butene, ethylene, and isobutene, which are generated

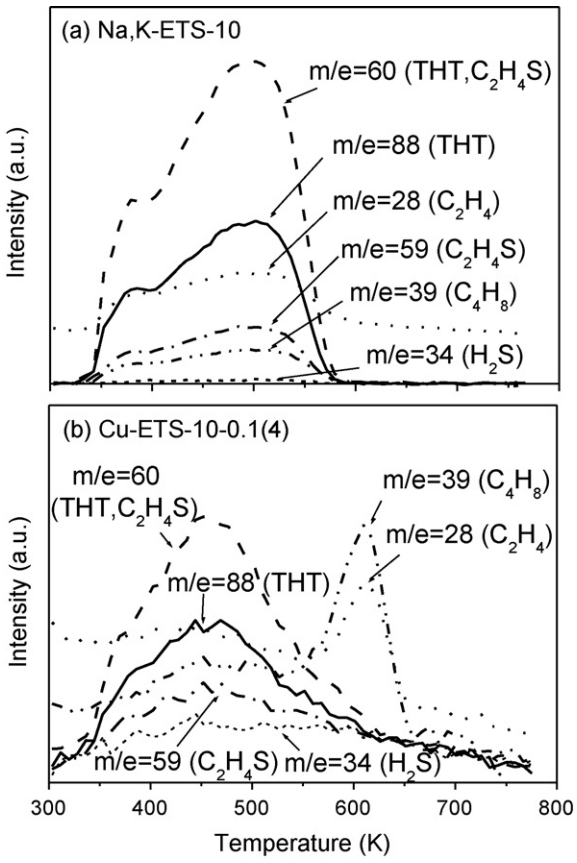


**Fig. 8.** The ionic current during TPD of THT adsorbed on (a) Na,K-ETS-10 and (b) Cu-ETS-10-0.1(4).

by the desulfurization of TBM and THT, can possibly transform to oligomeric species with a higher molecular weight on the copper active sites in Cu-ETS-10-0.1(4). Especially, in case of THT, the distribution of fragments on Cu-ETS-10-0.1(4) is different from that on Na,K-ETS-10. The intensities of ethylene ($m/e = 28$) and butene ($m/e = 39$, fragment of butene) peaks are relatively higher than that of THT ($m/e = 88$), as shown in Fig. 8. The results can be interpreted as that the desorption of sulfur compounds competes with their catalytic reaction on the copper active sites, and the catalytic process prevails against desorption process.

## 4. Conclusions

The ion exchange of Na(I) and K(I) of Na,K-ETS-10 with the Cu species was more effective in acidic condition, particularly pH at 4.0, than basic conditions, and the level of Cu incorporation increased with an increase in $Cu(NO_3)_2$ concentration in the ion exchange solution. A heat treatment of this ion exchanged Cu-ETS-10 at 723 K for 2 h in He atmosphere led to a partial auto-reduction of Cu(II) to Cu(I), which was confirmed by XPS.

On Na,K-ETS-10, the total uptakes for TBM and THT were 0.04 and 1.48 mmol S/g, respectively, with a much higher adsorption selectivity for THT over TBM. In a binary TBM and THT adsorption, posterior to the occurrence of breakthrough of TBM, THT adsorbed on the adsorption sites with desorption of TBM until THT occupied most of adsorption sites in Na,K-ETS-10. Noticeably on Cu-ETS-10, the breakthrough sulfur adsorption capacity for both TBM and THT was 2.50 mmol S/g with showing concurrent adsorption. This markedly high breakthrough sulfur adsorption capacity on Cu-ETS-10 was unprecedented in removing organic sulfur compounds from fuel gas by adsorption on zeolites. The introduction of copper in Na,K-ETS-10 made concurrent adsorption of TBM and THT without desorption of TBM during saturation.

Apparent activation energy for desorption of THT and TBM was an indirect indicative for their adsorption strength on the adsorption sites. The activation energy for desorption of TBM and THT adsorbed on Na,K-ETS-10 was 43.9 and 51.2 kJ/mol, respectively. This reflected that the adsorption strength of THT on Na,K-ETS-10 was higher than that of TBM, which led to preferential adsorption of THT over TBM on Na,K-ETS-10. The activation energy for desorption of TBM on Cu-ETS-10-0.1(4) was 53.0 kJ/mol, which was similar to that of THT (51.5 kJ/mol). This resulted in the concurrent adsorption of TBM and THT on Cu-ETS-10-0.1(4).

On Cu-ETS-10, the temperature of desorption peaks of TBM shifted largely into a higher temperature region, while that of THT shifted slightly into a lower temperature region than those on Na,K-ETS-10. These results reflected that the adsorption strength of TBM on Cu-ETS-10 was much higher than that in Na,K-ETS-10 and the adsorption strength of THT on Cu-ETS-10 was similar with that in Na,K-ETS-10. Thus, the increased adsorption strength of TBM on Cu-ETS-10 would be attributed to the concurrent adsorption of TBM and THT for sulfur adsorption with the binary TBM and THT feed stream.

## Acknowledgment

This study was supported by the Korea Research Foundation Grant (KRF-2005-042-D00075) founded by the Korean Government.

## References

[1] S.M. Haile, Acta Mater. 51 (2003) 5981.
[2] A. Rojey, M. Thoma, S. Jullian, US Patent Application 5,803,953 A1 (1998).
[3] L.J. Bonville, C.L. Degeorge, P.F. Foley, J. Garow, R.R. Lesieur, J.L. Preston, D.F. Szydlowski, US Patent No. 6,159,256 (2000).
[4] X. Ma, L. Sun, C. Song, Catal. Today 77 (2002) 107.
[5] P. Jeevanandam, K.J. Klabunde, S.H. Tetzler, Micropor. Mesopor. Mater. 79 (2005) 101.
[6] A. Takahashi, R.T. Yang, AIChE J. 48 (2002) 1457.
[7] S. Haji, C. Erkey, Ind. Eng. Chem. Res. 42 (2003) 6933.
[8] A.S.H. Salem, Ind. Eng. Chem. Res. 33 (1994) 336.
[9] R.T. Yang, A.J. Hernández-Maldonado, F.H. Yang, Science 301 (4) (2003) 79.
[10] M. Xue, R. Chitrakar, K. Sakane, T. Hirotsu, K. Ooi, Y. Yoshimura, Q. Feng, N. Sumida, J. Colloid Interf. Sci. 285 (2005) 487.
[11] S. Velu, X. Ma, C. Song, Ind. Eng. Chem. Res. 42 (2003) 5293.
[12] F.T.T. Ng, A. Rahman, T. Ohasi, M. Jiang, Appl. Catal. B: Environ. 56 (2005) 127.
[13] A.J. Hernández-Maldonado, R.T. Yang, AIChE J. 50 (4) (2004) 791.
[14] J. Weitkamp, M. Schwark, S. Ernst, J. Chem. Soc., Chem. Commun. (1991) 1133.
[15] C.L. Garcia, J.A. Lercher, J. Phys. Chem. 95 (1991) 10729.
[16] Y. Li, F.H. Yang, G. Qi, R.T. Yang, Catal. Today 116 (2006) 512.
[17] S. Satokawa, Y. Kobayashi, H. Fujiki, Appl. Catal. B: Environ. 56 (2005) 51.
[18] K.-I. Shimizu, N. Kobayashi, A. Satsuma, T. Kojima, S. Satakawa, J. Phys. Chem. B 110 (2006) 22570.
[19] I. Bezverkhyy, K. Bouguessa, C. Geantet, M. Vrinat, Appl. Catal. B: Environ. 62 (2006) 299.
[20] D.H. Lee, E.Y. Ko, H.C. Lee, S.H. Kim, E.D. Park, Appl. Catal. A: Gen. 334 (2008) 129.
[21] M.W. Anderson, O. Terasaki, T. Ohsuna, A. Philippou, S.P. Mackay, A. Ferreira, J. Rocha, S. Lidin, Nature 367 (1994) 347.
[22] J. Rocha, M.W. Anderson, Eur. J. Inorg. Chem. (2000) 801.
[23] Y.H. Kim, H.C. Woo, D.H. Lee, H.C. Lee, E.D. Park, Korean J. Chem. Eng. 26 (5) (2009) 1291.
[24] T.K. Das, A.J. Candwadkar, S. Sivasanker, Chem. Commun. (1996) 1105.
[25] P.A. Webb, C. Orr, Analytical Methods in Fine Particle Technology, Micromeritics Instrument Corporation, Norcross, 1997.
[26] W. Hidenobu, T. Yuko, H. Masato, Micropor. Mesopor. Mater. 46 (2001) 237.
[27] H.S. Kim, J.K. Chung, S.H. Lee, J.K. Cheon, M.J. Moon, H.C. Woo, Clean. Technol. 13 (2007) 64.
[28] R.J. Cvetanovic, Y. Amenomiya, Adv. Catal. 17 (1967) 103.
[29] S.M. Kuznicki, K.A. Thrush, US Patent Application 5,244,650 A1 (1993).
[30] A. Takahashi, F.H. Yang, R.T. Yang, Ind. Eng. Chem. Res. 41 (2002) 2487.